MEASUREMENTS ON THE FIRST SECTION OF THE SUPERCONDUCTING PROTON LINAC AT KARLSRUHE

J. L. Fricke, B. Piosczyk, J. E. Vetter
Institut für Experimentelle Kernphysik
Universität und Kernforschungszentrum
Karlsruhe, Germany

Abstract

The design of the first section of the proton linac at Karlsruhe, a resonator loaded with five electrically coupled helices, is described. Measurements of the first two test runs are presented. Results for quality factors and maximum obtained field strengths are given. Peak electric fields of 18 MV/m and corresponding peak magnetic fields of 530 Gauss were reached at $Q = 3.3 \times 10^7$. Field emission did not affect high field Q's significantly. This low β structure has accelerated protons with the design value of 1 MeV/m energy gain (particle phase = - 30°) in CW operation.

1. Introduction

The objectives of the Karlsruhe accelerator program are to show the feasibility of a superconducting π-meson factory by building a pilot proton accelerator (1). Parameter studies (1, 2) led to a concept to accelerate in a first step with helically loaded cavities at 90.5 MHz.

For the superconducting accelerator cooling considerations resulted in metallically supported λ/2-helices. A number of electrically coupled λ/2-helices in a common outer conductor form an accelerating section. The length of each section is given by focussing calculations.

Basic design parameters for the accelerator are injection energy of 0.75 MeV and frequency of 90.5 MHz. Because of the low particle velocity at injection energy ($\beta = 0.04$) the first helix section contains only five λ/2-helices which are driven in the π-mode.

Measurements on superconducting Nb-λ/2-helices on laboratory scale showed that accelerating fields of more than 1.2 MV/m can be obtained (3, 4, 5). So for the first helix section a design field on the axis of $E^{TW}_{axis} = 1.155$ MV/m was chosen, which corresponds to an energy gain of 1 MeV/m for a reference particle (particle phase = - 30°).

2. Apparatus

The geometry parameters of the first helix section resulted from calculations and measurements with room temperature models at Frankfurt and Karlsruhe. Starting with a modified **sheath model** (6) the ratios E^{max}/E^{TW}_{axis} and H^{max}/E^{TW}_{axis} were made as small as possible, because the application of rf superconductivity is limited in peak surface fields rather than in shuntimpedance. Other limitations, which had to be taken into account, were the maximum cooling capacity for a λ/2-helix (7) and minimum bending radius for the used Nb-tubes of 6.3 mm o. d.. This gave a first set of parameters for 5 coupled helices with a total electrical length of 36.8 cm. These parameters had to be corrected according to model measurements by A. Schempp (8), to allow for endfield effects, designed resonance frequency and to get an integer number of windings for technical reasons. This was done using an additional winding for the first and fifth helix and a higher phase velocity for the second and fourth helix in comparison with the sheath model values. The final parameters for the first section are given in Table I.

TABLE I

PARAMETERS OF THE FIRST SECTION

helix number	1	2	3	4	5
pitch / cm	0.97	1.01	1.05	1.09	0.99
radius / cm	4.15	4.0	4.15	4.03	3.75
number of windings	8	7	7	7	9

total length of the helix array 38.7 cm
total length of the tuned helix array 39.5cm

Due to mechanical tolerances it was necessary to retune the used Nb-helices in a room temperature model tank. In this tank it was possible to vary the helix position against each other for final frequency corrections and flatness. The field profile was checked with perturbation measurements. It was possible to get a field flatness better than ΔE/E = 5% over a mechanical length of 39.5 cm for the first helix section.

For the construction of the first section a mixed Pb/Nb-technique was used (3). The outer conductor was fabricated out of lead-plated electroformed copper with integrated cooling channels for the double vacuum system of the cryostat (9). The dimensions of the outer can are 40 cm i. d. and 54 cm length. We can use Pb for the superconducting outer conductor, because the field strengths at the surface of this outer conductor are only about 1% of the peak fields at the Nb-surfaces. The design of the cavity is shown in Figure 1. All Nb-parts were electron beam welded (electron beam welding was done by Siemens, Erlangen, Germany) to a single Nb-piece which is called

"Deckel" (10) (see Figure 1). In the middle of each helix, a coupling tube penetrates through the "Deckel", giving two movable and three fixed probes access to the E_r fields. The "Deckel" with the suspended helices is flanged into the lead-plated copper tank. Rf contact is made by a knife edge, whereas vacuum sealing at room temperature is achieved by a perbunan ring. The same kind of sealing is used to attach the endplates to the cylindrical part. The "Deckel" - filled with liquid helium and forming a helium bath for the suspended helices - is connected with the main helium reservoir of the crystat (9) within the twin pipes by two tubes with an inner diameter of 3 cm. Surface treatment was done by electropolishing (10) and anodizing (11, 12). Construction and preparation is described elsewhere (13) in considerable detail. Figure 2 shows the finished helix section mounted in the cryostat.

3. Results

The following results were obtained during two test runs.

TABLE II

DATAS OF THE TEST RUNS

TEST	A1	A2	B1	B2	B3
test dates	March-6 to March-17	March-20 to March-24	June-12 to June-17	June-20 to June-28	June-30 to July-7
preceeding treatments	fresh surface preparation	temperature cycling 1.8K-300K-1.8K	fresh surface preparation	temperature cycling 1.8K-77K-1.8K	temperature cycling 1.8K-300K-1.8K
$\max E^{TW}_{axis}$ [MV/m]	1.07 *	—	1.15 **	1.15 **	1.4 **
Q_o ($E^{TW}_{axis}=10^{-2}$ MV/m)	8.5×10^7	8.5×10^7	5.5×10^7	5.5×10^7	10×10^7
Q_o ($E^{TW}_{axis}=1$ MV/m)	3.3×10^7	—	1.1×10^7	1.1×10^7	3.3×10^7

* limited by thermal breakdown
** limited by 19Hz oscillation

Rf measurements were done as described in (3, 4) for λ/2 helices. Low power Q's were determined from decay time of stored energy. In the range of high power, Q-values were obtained by measuring the dissipated power in the cavity P_c and static frequency shift Δf_{stat}. The static frequency shift due to ponderomotive forces (14, 15) could be used for measuring stored energy as in the case of λ/2 helices (3, 4). Calibration measurements gave (Figure 3):

$$\Delta f_{stat}/\mathrm{kHz} = 5.7 \times 10^{-6} \times P_c Q_0'/\mathrm{watt} \qquad (1)$$

with an experimental error smaller than 5%. Q_0' includes coupling losses. The bead measurements, performed on this helix section at room temperature, resulted in:

$$E^{TW}_{axis}/\mathrm{MV/m} = 1.05 \times 10^{-4}\sqrt{P_c Q_0'/\mathrm{watt}} \qquad (2)$$

(neglecting the end effects).

The estimated error in E is 5%. With equ. (1) and (2) one gets:

$$E^{TW}_{axis}/\mathrm{MV/m} = 4.38 \times 10^{-2}\sqrt{\Delta f_{stat}/\mathrm{kHz}} \qquad (3)$$

The design field of E^{TW}_{axis} = 1.155 MV/m corresponds to Δf_{stat} = 696 kHz (equ. (3)).

Peak fields were calculated according to the ring model for long helices (16). The relations between peak fields and accelerating fields are given in Table III.

TABLE III

PEAK FIELDS RELATED TO THE ACCELERATING FIELD STRENGTH E^{TW}_{axis}

helix No.	$E_z^{max}/E^{TW}_{ax.}$	$E_r^{max}/E^{TW}_{ax.}$	$H_r^{max}/E^{TW}_{ax.}$	$H_z^{max}\ E^{TW}_{ax.}$
1	11.64	6.77	334	277
2	12.85	7.77	378	309
3	11.62	7.53	340	299
4	10.61	7.33	309	293
5	9.10	5.81	247	251

$$[E] = [\mathrm{MV/m}] \qquad [H] = [\mathrm{Gauss}]$$

For the designed accelerating field strength of E^{TW}_{axis} = 1.155 MV/m we get maximum surface fields of E_z^{max} = 15 MV/m and H_r^{max} = 437 Gauss. Quality-factors are plotted versus accelerating field strength for several test runs in Figure 4. The main dependencies of Q (E) are the same as in λ/2 helices (3, 4). The reentrant cavities at Stanford (350 MHz) showed deteriorated Q-values at high field levels too (17). So the reason for this behaviour can not be the special kind of cavity only, but might be a property of the low frequency.

The high field Q-value saturates at $Q = 3.3 \times 10^7$ in period B1 and B3, and is about a factor of 3 lower than in single helix experiments. This value corresponds to an improvement factor of 2×10^4 compared to room temperature copper. Looking at the high field Q's of experiment A1 and B3 (Figure 4) one would expect similar breakdown mechanism in both cases. Experiment A1 showed thermal breakdown at Δf_{stat} = 600 kHz at a power loss near to the upper limit of helix cooling capacity of about P_c = 3.25 watts for these helix dimensions (7). Though P_c was 7 watts in period B3 no thermal breakdown was to be seen up to Δf_{stat}=994kHz. Limitation of field strength was due to a

mechanical 19 Hz oscillation of the helix array enhanced by ponderomotive forces (13, 15). In the 103 MHz mode (see chapter 4) one could handle a P_c = 25 watts without breakdown. A thermometer at the outer conductor showed a temperature rise with rf power. Temperature instabilities were seen at P_c values exceeding 4 watts. We conclude from this that the dominant losses in B3 occured either on the cylindrical part of the outer conductor or in its joint to the niobium "Deckel".

In period A2, the Q-values of A1 were reproduced. Due to an accidental vacuum breakdown, the Q-values deteriorated at the end of period B2. It was gratifying to note that after warming up to room temperature, pumping and cooling down again the high field Q was not only restored, but even improved by a factor of 3 (Figure 4). A reason for this improvement might be the different expansion coefficients of copper and niobium resulting in a change of rf contact in temperature cycling.

In period A1 a field of E^{TW}_{axis} = 1.07 MV/m could be handled in stable operation, which is near to the design field strength. In the second run (B1-B3) the initial limitation of field strength by ponderomotive oscillation could be overcome using a coupling between frequency and amplitude controls (13, 15). In this way we got stable operation for hours at an accelerating field of 1.3 MV/m. At the maximum frequency shift of 994 kHz stability still persisted. This corresponds to an accelerating field of E^{TW}_{axis} = 1.4 MV/m and peak fields of E_z^{max} = 18 MV/m and H_φ^{max} = 530 Gauss.

During the experimental periods we had some trouble with electron loading of the section. In every test run, which was started from room temperature, we got multipactor barriers. We could overcome them by "processing" with high rf power (3, 4). A barrier from Δf_{stat} = 25 kHz to Δf_{stat} = 105 kHz took about 15 hours processing time. The measured r-factor (18) was about 100, indicating one point multipacting.

Though field emission started like for λ/2 helices at 14 MV/m (3, 4), it did not affect Q-values of the cavity. A Fowler Nordheim plot (19) yielded an enhancement factor of 320 (B3), similar to the λ/2 helices. The electron bombardment decoulored the Nb_2O_5 surface layer of the helices in some regions of high fields.

Mechanical oscillations excited by external forces, like the vacuum pumps or the refrigerator, modulate the resonant frequency of the cavity. So the dynamical phase error between adjacent helices was measured, an effect that would influence beam dynamics. Using fixed coupling probes (coupling factor $\beta << 1$) it was only possible to measure a superposition of the E_r fields of adjoined helices. Though the helices were driven in the π-mode, the phase between two cells wasn't 180°. To exclude errors in dynamical phase measurement caused by the effect described above, we used different combinations of the coupling probes. The phase error between adjacent helices was smaller than 0.1° at an external vibration level of 24 kHz_{pp} (period A1) and smaller than 0.4° at an enhanced vibration level of 150 kHz_{pp} (period B3).

It was also checked, that the phase between adjacent helices did not change with field level. We conclude that the static frequency shift (equ. (3)) does not affect the mode.

4. Measurements with beam

All acceleration measurements were done with a dc beam, because the buncher was defect, due to a trivial failure (13). We did not use an rf amplitude regulation system. So we were forced to use beam currents lower than 10 μA because of a 20% beam intensity modulation caused by a defect of the duoplasma source of the injector. The type of coupling (see chapter 2) limited the beam current to about 25 μA for a bunched beam. In the future stronger coupling (20) will be used for experiments with higher beam currents and phasing of two or more cavities.

The energy gain as a function of field strength in the helix resonator and as a function of injection energy was measured. The results are summarized in Figure 5. The design field of 1.155 MV/m gave a maximum energy gain of 380 keV at 750 keV injection energy. At the same injection energy and a field strength of 1.35 MV/m we measured 452 keV maximum energy gain.

According to the calculated sheath model parameters (chapter 2) the total electrical length of the first helix section is 36.8 cm. Using this length a maximum energy gain (particle phase = 0°) of 424 keV and 497 keV is calculated for accelerating field strengths of 1.155 MV/m and 1.35 MV/m, respectively. This calculated values for the energy gain are systematically higher than the measured ones. The reason for this discrepancy is a final mechanical length of the helix section of 39.5 cm instead of the corrected sheath model length of 38.7 cm (Table I). We arrived at 39.5 cm total length by final mechanical adjustments to get the right frequency, and field flatness smaller than 5%. For a better comparison between experimental energy gain and calculated values the following method was used. From the field pattern on the axis of the accelerating section as measured by bead measurements the energy gain of particles can be calculated with a computer program (21). The measured values fit well to the calculated numbers within the limits of experimental error (10% of the particle energy). They are plotted in Figure 5.

Varying the injection energy we

could see that the accelerator section has nearly the same energy gain for a wide range of injection energies.

A test was carried out with a dc-beam of 1.3 μA at an injection energy of 750 keV in test B3. The beam was accelerated at a field level of 1.3 MV/m for 3 1/2 hours.

Test on non-resonant beam loading phenomena were done according to a method from an electron analog experiment (22). The first helix section has five fundamental modes in the lowest passband:

90, 94, 103, 120, 136 MHz.

Due to the geometry of the helix, the transverse modes are in the GHz region and so we only expect longitudinal beam loading effects. If the helix section is driven in the π-mode (lowest frequency in a backward wave structure) the phase velocities of all other fundamental modes in the lowest passband are higher than the phase velocity of the π-mode, which is made equal to the velocity of the particles. Therefore these modes cannot be excited by the beam. In a non-ideal structure each mode has an infinite number of space harmonics. So it is possible to excite those space harmonics which have phase velocities slightly lower than the velocity of the particles. First we looked for excitation of the 94 MHz and 103 MHz mode. No excitation could be seen up to beam currents of 0.5 mA. The results are still qualitative and are to be completed by further measurements.

5. Summary

We reached sufficient Q-values of 3.3×10^7 (up to $E^{TW}_{axis} = 1.4$ MV/m in B3) in two different test runs with fresh preparation in between, using a surface preparation similar to λ/2 helices.

Vacuum breakdown deteriorated Q-values and obtainable field strengths. But after temperature cycling to room temperature and evacuating the structure, the original values were restored.

We operated the section with an 1.3 μA proton beam at a field level of 1.3 MV/m, which is higher than the design value of $E^{TW}_{axis} = 1.155$ MV/m

A maximum accelerating field of 1.4 MV/m could be handled in stable operation limited by the rf control curcuit.

No non-resonant beam loading was observed up to beam currents of 0.5 mA.

Acknowledgments

The performance of the accelerator test was done with the aid of the whole accelerator group at Karlsruhe. The authors thank H. Klein and his group at Frankfurt for calculating the parameters of the section.

References

(1) A. Citron, Proc. 1970 Proton Lin. Acc. Conf. NAL Batavia, Vol. I, 239 (1970)
(2) H. Klein and O. Siart, Proc. 1970 Proton Lin. Acc. Conf. NAL Batavia, Vol.I, 293 (1970)
(3) J. L. Fricke, B. Piosczyk, J. E. Vetter and H. Klein, Particle Accelerators, 3, 35 (1972)
(4) A. Citron, J. L. Fricke, C. M. Jones, H. Klein, M. Kuntze, B. Pioszyk, D. Schulze, H. Strube, J. E. Vetter, N. Merz, A. Schempp and O. Siart, Proc. 8th Int. Conf. on High Energy Accelerators, CERN, 1971, p. 278
(5) R. Benaroya, A. H. Jaffey, K. Johnson, T. Khoe, J. J. Livingood, J. M. Nixon, G. W. Parker, W. J. Ramler, J. Aronand, W. A. Wesolowski, Appl. Phys. Letters, 21, No. 5, 235 (1972)
(6) H. Klein, N. Merz, O. Siart, Part. Acc. 4, to be published
(7) G. Krafft, Proc. 4th Int. Cryogenic Engineering Conf., ICEC4, Eindhoven 1972 (in press)
(8) A. Schempp, Bericht No. 12, Institut für angewandte Physik, Universität Frankfurt, Germany 1971 (unpublished)
(9) W. Barth, P. Flécher, F. Graf, M. A. Green, W. Herz, L. Hütten, H. Katheder, W. Lehmann, F. Spath, G. Winkler, Proc. 4th Int. Cryogenic Engineering Conf., ICEC 4, Eindhoven 1972 (in press)
(10) H. Diepers, O. Schmidt, and H. Martens, Phys. Letters A 37, 139 (1971)
(11) H. Martens, H. Diepers, and R.K. Sun, Phys. Letters A 34, 439 (1971)
(12) P. Kneisel, O. Stoltz, J. Halbritter IEEE Trans. Nucl. Sci NS-18, No. 3, 159 (1971)
(13) A. Brandelik, P. Flécher, J. L. Fricke, J. Halbritter, R. Hietschold, G. Hochschild, G. Hornung, H. Klein, P. Kneisel, G. Krafft, W. Kühn, M. Kuntze, B. Piosczyk, E. Sauter, A. Schempp, D. Schulze, L. Szecsi, J. E. Vetter, K. W. Zieher (submitted to Particle Accelerators)
(14) D. Schulze, KFK-Bericht 1493, KFZ Karlsruhe (1971)
(15) D. Schulze (this Conference)
(16) O. Siart, Thesis, Universität Frankfurt (1970)
(17) I. Ben-Zwi, J. G. Castle, jr., and Peter H. Ceperly, IEEE Trans. Nucl. Sci. NS-19, No. 2, April 1972
(18) J. Halbritter, Part. Acc. 3, 163 (1972)
(19) H. Schopper, H. Strube, and L. Szecsi
(20) J. E. Vetter, KFZ Karlsruhe, internal Note 189 (unpublished), 1972
(21) W. Jüngst, M. Kuntze, and J. Vetter, Ext. Report 3/67-15, KFZ, Karlsruhe
(22) K. Mittag, Ext. Report 3/69-29, KFZ Karlsruhe, 1969)

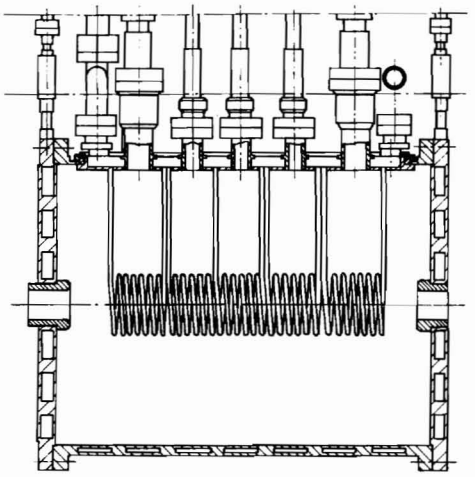

Fig. 1 Design of the first section

Fig. 2 View of the section mounted in the cryostat

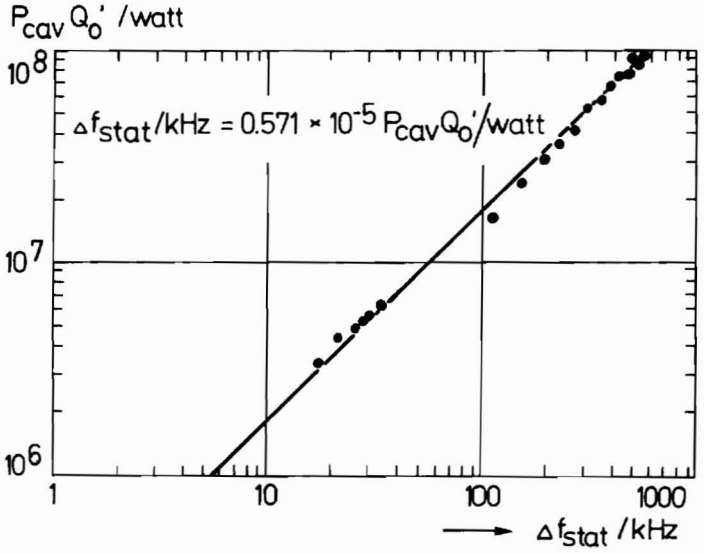

Fig. 3 PcQ_0' as a function of static frequency shift Δf_{stat}

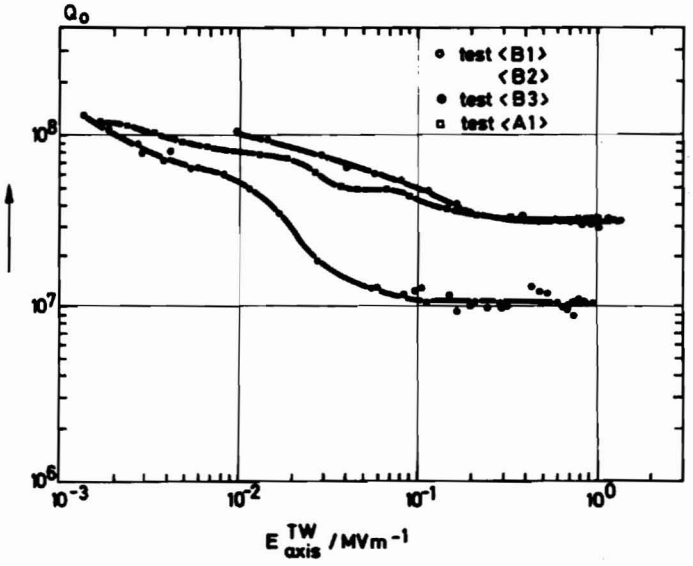

Fig. 4 Q_0 values as a function of accelerating field strength E^{TW}_{axis}

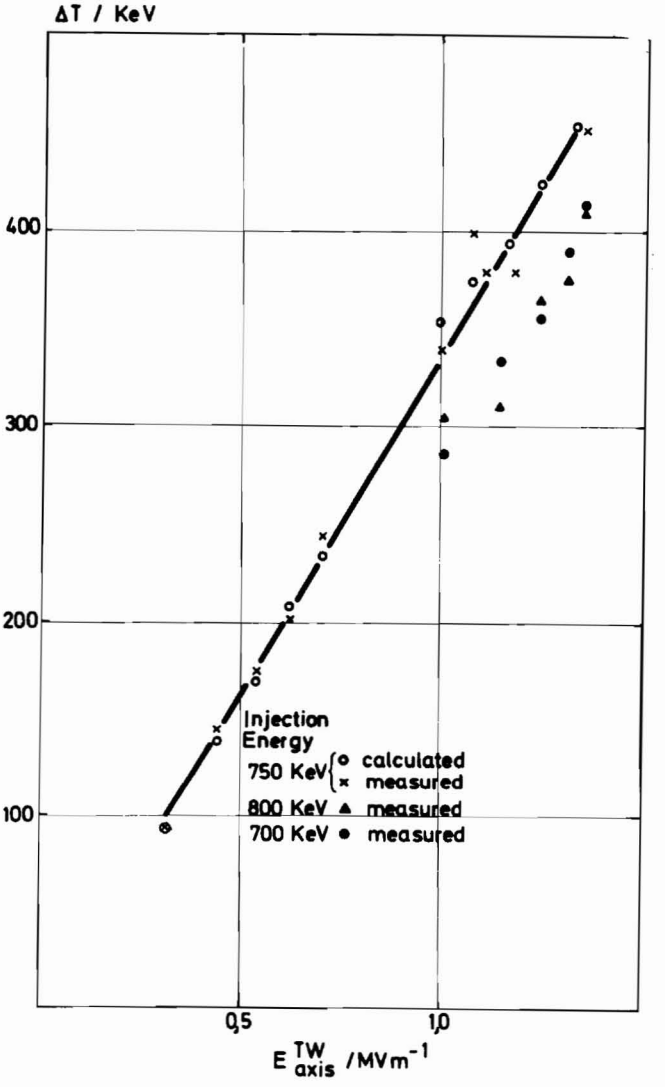

Fig. 5 Measured and calculated energy gain ΔT as a function of accelerating field strength